

Dynamic charge inhomogeneity in cuprate superconductors

This article has been downloaded from IOPscience. Please scroll down to see the full text article.

2010 J. Phys.: Condens. Matter 22 142201

(<http://iopscience.iop.org/0953-8984/22/14/142201>)

View [the table of contents for this issue](#), or go to the [journal homepage](#) for more

Download details:

IP Address: 129.252.86.83

The article was downloaded on 30/05/2010 at 07:42

Please note that [terms and conditions apply](#).

FAST TRACK COMMUNICATION

Dynamic charge inhomogeneity in cuprate superconductors

Thomas Bauer and Claus Falter

Institut für Festkörperteorie, Westfälische Wilhelms-Universität, Wilhelm-Klemm-Straße 10,
48149 Münster, GermanyE-mail: falter@uni-muenster.de

Received 1 February 2010, in final form 26 February 2010

Published 17 March 2010

Online at stacks.iop.org/JPhysCM/22/142201**Abstract**

The inelastic x-ray scattering spectrum for phonons of Δ_1 symmetry, including the CuO bond-stretching phonon dispersion, is analyzed by means of Lorentz fitting for $\text{HgBa}_2\text{CuO}_4$ and $\text{Bi}_2\text{Sr}_2\text{CuO}_6$, using recently calculated phonon frequencies as input parameters. The resulting mode frequencies of the fit are almost all in good agreement with the calculated data. An exception is the case for the second-highest Δ_1 branch compromising the bond-stretching modes, which disagrees for both compounds with the calculations. This branch shows an anomalous softening with a minimum around the wavevector $\mathbf{q} = \frac{2\pi}{a}(0.25, 0, 0)$, at variance with the calculation predictions. Such a disparity with the calculated results, that are based on the assumption of an undisturbed translation and point group invariant electronic structure of the CuO plane, indicates some *static* charge inhomogeneities in the measured probes. Most likely these will be charge stripes along the CuO bonds which have the strongest coupling to certain longitudinal bond-stretching modes, that in turn self-consistently induce corresponding *dynamic* charge inhomogeneities. The symmetry breaking by the mix of dynamic and static charge inhomogeneities can lead to a reconstruction of the Fermi surface into small pockets.

In recent work [1, 2] the IXS phonon spectra of optimally doped $\text{HgBa}_2\text{CuO}_4$ and $\text{Bi}_2\text{Sr}_2\text{CuO}_6$ have been measured for the Δ_1 symmetry modes. The spectra have been interpreted by using a Voigt fit function. For the interesting high frequency part of the spectra where the CuO bond-stretching modes (BSM) are expected that are known to display an anomalous softening upon doping in the cuprates [3–12], only one phonon peak has been fitted in the case of $\text{HgBa}_2\text{CuO}_4$ [1] and two in the case of $\text{Bi}_2\text{Sr}_2\text{CuO}_6$ [2].

On the other hand, from our microscopic calculation of the phonon dynamics of $\text{HgBa}_2\text{CuO}_4$ and $\text{Bi}_2\text{Sr}_2\text{CuO}_6$ [13] we find in the high energy region of the IXS spectra along $\frac{2\pi}{a}(\zeta, 0, 0)$ up to four Δ_1 modes as far as $\text{HgBa}_2\text{CuO}_4$ is concerned and up to five Δ_1 modes in $\text{Bi}_2\text{Sr}_2\text{CuO}_6$. These modes interact strongly with each other and constitute a highly nontrivial anticrossing scenario. As a consequence a multiple-mode fit is necessary for obtaining more reliable results. The strength of the measured peaks strongly decreases for larger ζ values such that at $\zeta \approx 0.5$ the peaks are very weak (see e.g. figure 1), and a unique interpretation taking only one or two peaks into

account is incomplete because of the many modes of the same symmetry in this region of energy. Nevertheless, it is very interesting that in the limited Voigt fit of the spectra in [1, 2] a hint of an anomalous softening of the BSM dispersion is extracted at $\zeta \approx 0.3$ for the Hg compound and at $\zeta \approx 0.25$ for the Bi compound. Such an enhanced softening at these ζ values has not been detected in our calculations for the Δ_1 modes. Only the presumably generic softening in the cuprates of the half-breathing mode (HBM) in $\text{HgBa}_2\text{CuO}_4$ and of two half-breathing modes in $\text{Bi}_2\text{Sr}_2\text{CuO}_6$, generated by the strong nonlocal electron–phonon interaction (EPI) mediated by the charge fluctuations (CF) on the outer electron shells of the ions, has been found in our calculations [13].

In the presence of these theoretical results and the complex anticrossing of the Δ_1 modes it is very desirable to perform a more complete analysis of the IXS measurements on the basis of the calculation of the dispersion of the Δ_1 modes as given in [13]. In such a reconstruction of the IXS phonon spectra we do not apply the more complicated Voigt fit but use instead a simpler Lorentz fit function, which does the job very well. This

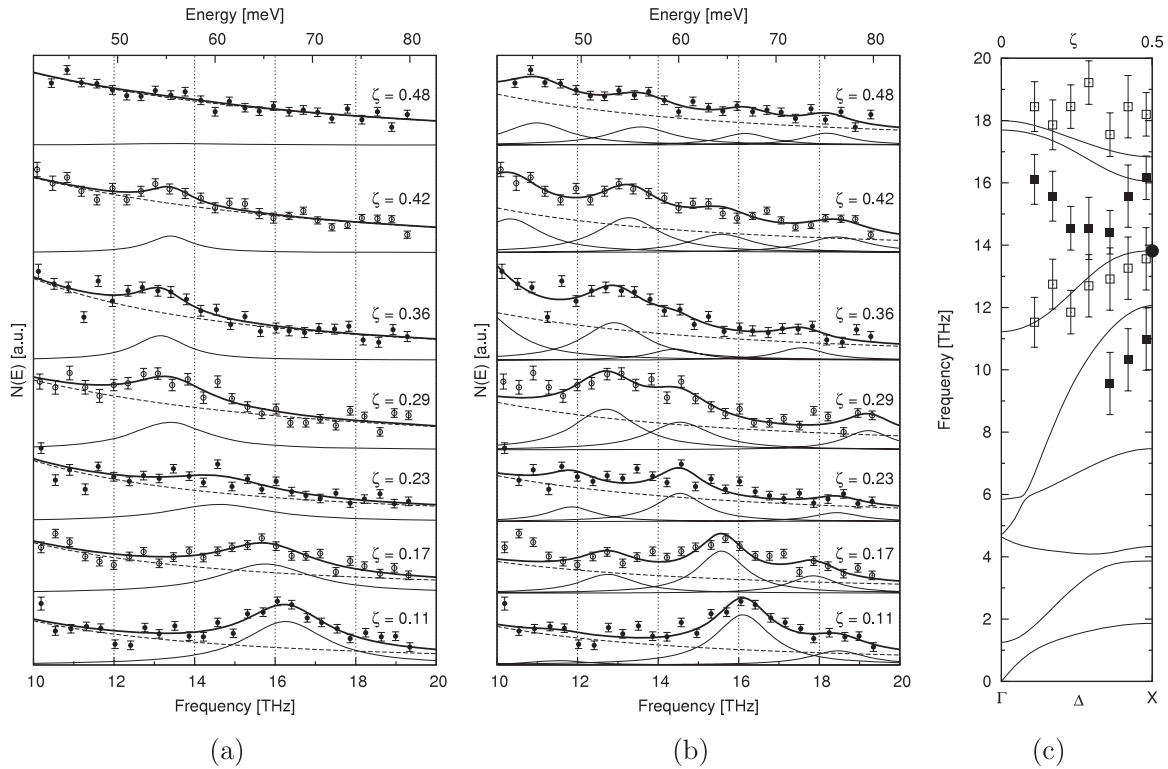


Figure 1. (a) Reconstructed IXS phonon spectrum of $\text{HgBa}_2\text{CuO}_4$ from [1] for $\mathbf{q} = \frac{2\pi}{a}(\zeta, 0, 0)$ using a Lorentz fit with one mode only (thick line); the corresponding Lorentz peaks of the modes are also shown (thin line). The broken line represents the elastic background. The inelastic cross section $N(E)$ is given in arbitrary units. (b) The same as (a) but using a Lorentz fit on the basis of the calculated phonon dispersion for modes of Δ_1 symmetry in the energy range considered [13]. (c) Calculated phonon dispersion of $\text{HgBa}_2\text{CuO}_4$ for modes of Δ_1 symmetry according to [13]. The symbols \blacksquare and \square denote the phonon frequencies from the Lorentz fit and \bullet the half-breathing mode. The vertical bars indicate the FWHM of the peaks determined in the fitting.

can be concluded from figure 1(a) where the IXS spectrum of $\text{HgBa}_2\text{CuO}_4$ [1] is reconstructed for $\mathbf{q} = \frac{2\pi}{a}(\zeta, 0, 0)$ using, as in [1], only one peak in the Lorentz fit. The phonon frequencies fitted at $\zeta = 0.11, 0.17, 0.23, 0.29, 0.36, 0.42$ and 0.48 are 16.28 (16.32), 15.76 (15.73), 14.61 (14.65), 13.38 (13.73), 13.15 (13.14), 13.40 (13.53) and 13.51 (13.63) THz. The data within the brackets are the frequencies as obtained from the Voigt fit [1]. We recognize a very good agreement between the results from the two fitting procedures. As far as $\text{Bi}_2\text{Sr}_2\text{CuO}_6$ is concerned we also get nearly indistinguishable results for a two-mode fit in the two fitting schemes, so we take the simpler Lorentz fit in this work.

In figure 1(b) we present the results of the Lorentz fit for the analysis of the IXS spectrum of $\text{HgBa}_2\text{CuO}_4$ within the framework of the calculated Δ_1 modes in the relevant energy range [13]. As already mentioned, up to four mode frequencies must be considered. The calculated frequencies at the corresponding ζ values are taken as input parameters of the Lorentz fit. From the results displayed in figure 1(b) we find that the IXS spectrum is well represented by the multiple-mode fit. The Lorentz peaks as obtained from the fit are also shown in the figure for each ζ value.

The resulting phonon frequencies from the fit are shown in figure 1(c) together with the calculated dispersion of the Δ_1 modes [13]. Except for the second-highest Δ_1 branch comprising the BSM, that displays anomalous softening

starting at $\zeta \approx \frac{1}{8}$ with a minimum around $\zeta = \frac{1}{4}$, the resulting mode frequencies are in reasonable agreement with the calculated branches.

For the case of $\text{Bi}_2\text{Sr}_2\text{CuO}_6$, the Lorentz fit of the IXS spectrum obtained on the basis of the calculated Δ_1 modes [13] is shown in figure 2(b) and likewise, as for $\text{HgBa}_2\text{CuO}_4$, a good resolution of the spectrum is achieved. The extracted phonon frequencies from the fit are shown in figure 2(c). For comparison the calculated dispersions of the Δ_1 modes [13] are displayed in the figure. Leaving aside the second-highest branch, we find a good agreement of the calculated branches with the modes from the Lorentz fit. As for $\text{HgBa}_2\text{CuO}_4$, the second-highest Δ_1 branch displays an anomalous softening starting at $\zeta \approx \frac{1}{8}$ with a minimum around $\zeta = \frac{1}{4}$.

Strong coupling of the BSM with dynamic charge stripes generated self-consistently, via strong nonlocal electron-phonon interaction (EPI), by the BSM themselves leading to an anomalous softening has already been found earlier for the cuprate-based superconductors for the case of an undisturbed translation and point group invariant electronic structure of the CuO plane without any charge inhomogeneities [14–19]. The same holds true for $\text{HgBa}_2\text{CuO}_4$ and $\text{Bi}_2\text{Sr}_2\text{CuO}_6$ as can be seen from the calculations in this work displayed in figure 3, where the charge redistribution $\delta\rho(\mathbf{r})$ for the half-breathing mode (HBM) ($\zeta = \frac{1}{2}$) induced by nonlocal EPI is shown. In the HBM propagating in the $\Delta \sim (1, 0, 0)$ direction the O_x

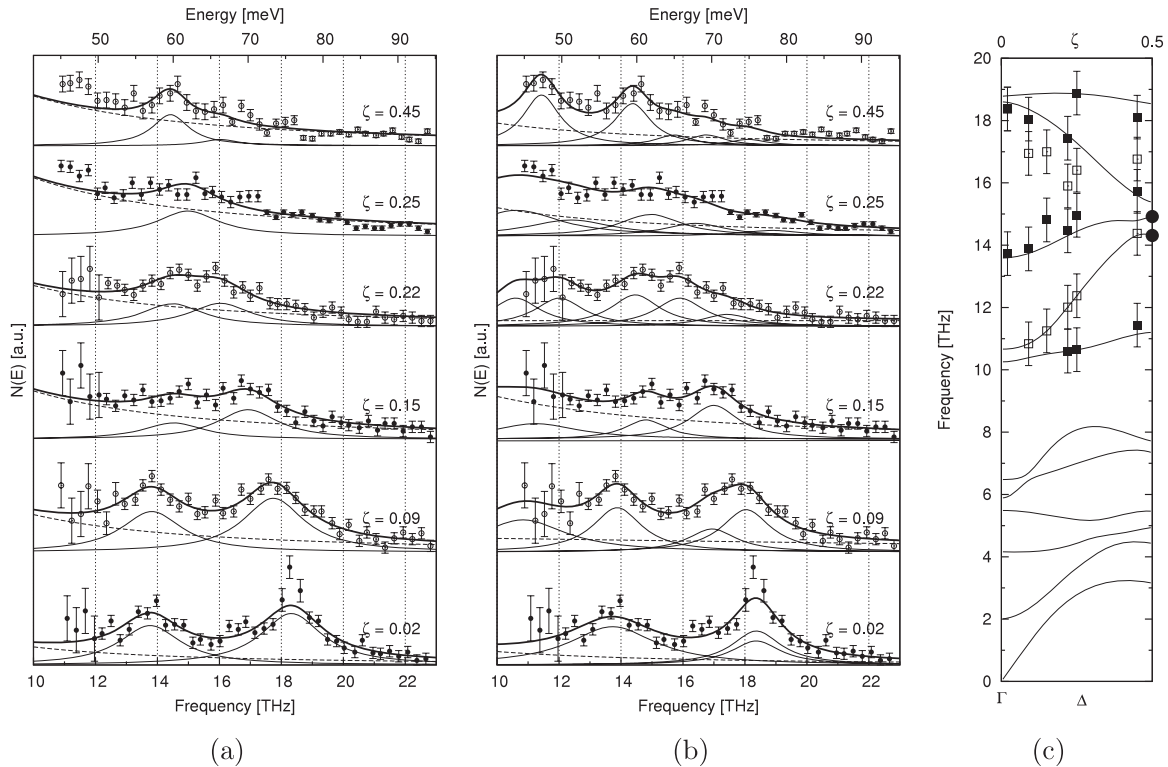


Figure 2. (a) Reconstructed IXS phonon spectrum of $\text{Bi}_2\text{Sr}_2\text{CuO}_6$ from [2] for $\mathbf{q} = \frac{2\pi}{a}(\zeta, 0, 0)$ obtained using a Lorentz fit with two modes only (thick line); the corresponding Lorentz peaks of the modes are also shown (thin line). The broken line represents the elastic background. The inelastic cross section $N(E)$ is given in arbitrary units. (b) The same as (a) but using a Lorentz fit on the basis of the calculated phonon dispersion for modes of Δ_1 symmetry in the energy range considered [13]. (c) Calculated phonon dispersion of $\text{Bi}_2\text{Sr}_2\text{Cu}_6$ for modes of Δ_1 symmetry according to [13]. The symbols \blacksquare and \square denote the phonon frequencies from the Lorentz fit and \bullet the half-breathing modes. The vertical bars indicate the FWHM of the peaks determined in the fitting.

ions move coherently along the CuO bond towards or away from the silent Cu ion. For the detailed displacement pattern, see [13].

Figure 3 illustrates that the HBM creates in both compounds dynamic charge ordering $\delta\rho$ via charge fluctuations at the ions due to nonlocal EPI in the form of localized stripes of alternating sign in the CuO plane. The period of the pattern is twice the lattice constant for $\zeta = \frac{1}{2}$. In the case of $\text{Bi}_2\text{Sr}_2\text{CuO}_6$ these dynamic charge inhomogeneities are only shown for one of the two HBM modes found in the calculations, namely the one with the lower frequency (see figure 2(c)), because the charge redistribution is very similar for the other HBM. For $\text{HgBa}_2\text{CuO}_4$ we obtain only one HBM (see figure 1(c)), which induces the dynamic stripe pattern in figure 3(b). In the HBM the dynamic charge stripes point along the x - or y -axis, respectively, if the oxygen ions move along the CuO bond in the y - or x -direction, respectively.

It should be noted that for the oxygen breathing mode at the X point (see [13]), the dynamic stripes excited point along the diagonals of the CuO plane. Furthermore, it should be remarked that dynamic charge inhomogeneities like the dynamic stripe patterns would not be present in systems with only *local* EPI at work, for example, in a high density homogeneous electron gas prevailing in simple metals. This is because of perfect screening of the changes of the Coulomb potential related to the displacement of the ions in a phonon

mode. On the other hand, our calculations exhibit a strong nonlocal EPI in the cuprates essentially due to the poor screening in these materials with a large component of ionic binding; see e.g. [19]. This demonstrates the special role of a strong nonlocal EPI for the physics of these compounds in their normal as well as in the superconducting state.

Such a strong coupling is also underlined by recent experimental results for the quasi-particle dispersion in $(\text{Bi, Pb})_2\text{Sr}_2\text{CuO}_{6+\delta}$ [20]. The super-high resolution laser-based angle-resolved photoemission spectroscopy measurements reported in [20] show unambiguously that the ~ 70 meV nodal kink in the dispersion is due to strong EPI with multiple phonon modes as seen in the Eliashberg spectral function extracted from the measured real part of the electron self-energy. Remarkably, the peak structure of the Eliashberg function is in very good agreement with our calculated phonon density of states for $\text{Bi}_2\text{Sr}_2\text{CuO}_6$ [13]; see figure 4.

Quite generally, our calculations for the cuprates demonstrate the enhanced affinity of the BSM to induce dynamic charge inhomogeneities in the form of stripes in the CuO plane. So, it can be safely argued that the latter will also occur in a modified way in systems with static stripe charge order breaking translation and point group invariance. The anomalous softening around $\zeta = \frac{1}{4}$ found by the analysis of the IXS phonon spectra then reflects the strong nonlocal coupling of the BSM with their self-consistently induced

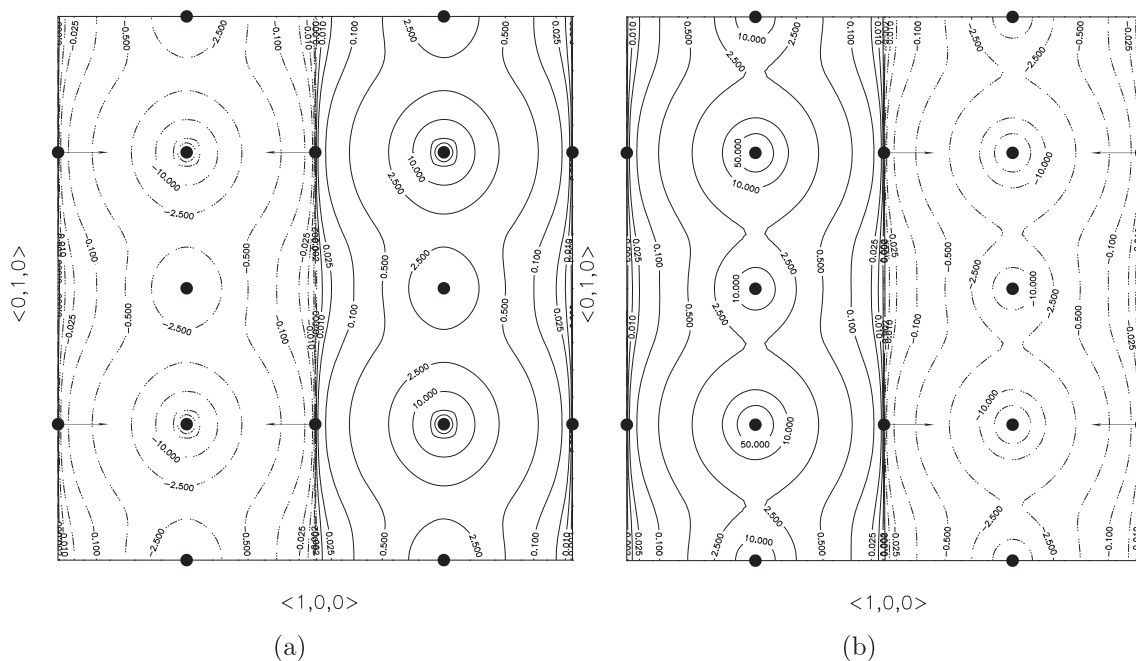


Figure 3. Dynamical charge stripes $\delta\rho$ as induced by the half-breathing mode (with the lower frequency) in $\text{Bi}_2\text{Sr}_2\text{CuO}_6$ (a) and in $\text{HgBa}_2\text{CuO}_4$ (b). The arrows indicate the vibrating oxygen ions. Units are $10^{-4} e^2/a_B$. Regions of space where electrons are accumulated are characterized by full lines and those where electrons are pushed away by broken dotted lines.

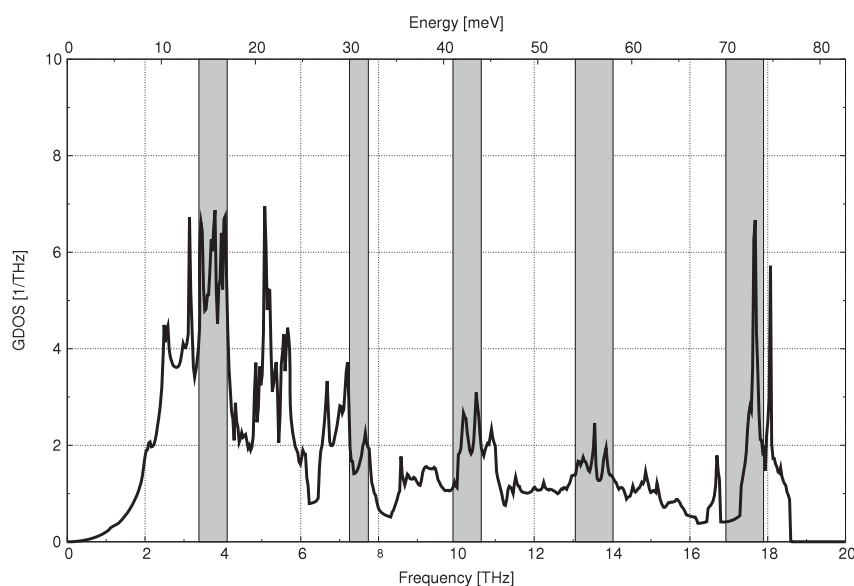


Figure 4. Calculated phonon density of states for $\text{Bi}_2\text{Sr}_2\text{CuO}_6$. The gray domains mark the peaks of the Eliashberg spectral function [20].

dynamic charge inhomogeneities (dynamic stripes) but now in probes with a static charge inhomogeneity (static stripes) presumably present. Excess holes in a stripe will even enhance the strong nonlocal coupling to the BSM and consequently also the magnitudes of the CFs, and the related mode softening is increased. An interrelation between the number of holes and softening is supported by the experiment and our calculations for the Cu–O bond-stretching modes [14, 15].

The symmetry breaking of the electronic structure by charge inhomogeneity in the form of static stripe patterns accompanied by phonon-induced dynamic fluctuating patterns

shown by our calculations to occur very likely may lead to a corresponding reconstruction of the Fermi surface into small pockets. This reconstruction is in turn the origin for the quantum oscillations in some cuprates that have been measured; see e.g. [21]. In this context it is interesting that in [22] the quantum oscillations are attributed to symmetry breaking by a certain type of stripe order in the form of a combined charge/spin modulation. Other authors attribute the small Fermi surface pockets to magnetic fluctuations [23], to density waves [24] or to antiferromagnetic (π, π) spin density waves [25].

Finally, it should be added that in the literature, dynamic charge inhomogeneities related to electron–phonon coupling are discussed from the experimental side for $\text{La}_{2-x}\text{Ba}_x\text{CuO}_4$, $\text{YBa}_2\text{Cu}_3\text{O}_7$ or $\text{Ba}_{0.6}\text{K}_{0.4}\text{BiO}_3$ in [26–33] and from the theoretical side e.g. in [34].

In summary, our analysis of the IXS phonon spectra for $\text{HgBa}_2\text{CuO}_4$ and $\text{Bi}_2\text{Sr}_2\text{CuO}_6$ within the framework of calculated phonon dispersion curves points to the existence of dynamic charge inhomogeneities generated by the BSM via strong nonlocal EPI of the CF type. These modes excite dynamic charge order and consequently can also serve as indirect probes for corresponding static charge order in the cuprates. Thus, we have a mix of static and fluctuating charge order in the materials.

References

- [1] Uchiyama H *et al* 2004 *Phys. Rev. Lett.* **92** 197005
- [2] Graf J *et al* 2008 *Phys. Rev. Lett.* **100** 227002
- [3] Pintschovius L 2005 *Phys. Status Solidi b* **242** 30
- [4] Pintschovius L and Reichardt W 1998 *Neutron Scattering in Layered Copper-Oxide Superconductors (Physics and Chemistry of Materials with Low Dimensional Structures vol 20)* ed A Furrer (Dordrecht: Kluwer–Academic)
- [5] Pintschovius L and Braden M 1999 *Phys. Rev. B* **60** R15039
- [6] Reichardt W 1996 *J. Low Temp. Phys.* **105** 807
- [7] Fukuda T *et al* 2005 *Phys. Rev. B* **71** R060501
- [8] Pintschovius L *et al* 2006 *Phys. Rev. B* **74** 174514
- [9] McQueeney R J *et al* 2001 *Phys. Rev. Lett.* **87** 077001
- [10] d’Astuto M *et al* 2002 *Phys. Rev. Lett.* **88** 167002
- [11] d’Astuto M *et al* 2003 *Int. J. Mod. Phys. B* **17** 484
- [12] Braden M *et al* 2005 *Phys. Rev. B* **72** 184517
- [13] Bauer T and Falter C 2010 *J. Phys.: Condens. Matter* **22** 055404
- [14] Falter C 2005 *Phys. Status Solidi b* **242** 78
- [15] Falter C, Bauer T and Schnetgöke F 2006 *Phys. Rev. B* **73** 224502
- [16] Falter C *et al* 1997 *Phys. Rev. B* **55** 3308
- [17] Bauer T and Falter C 2008 *Phys. Rev. B* **77** 144503
- [18] Falter C and Hoffmann G 2000 *Phys. Rev. B* **61** 14537
- [19] Bauer T and Falter C 2009 *Phys. Rev. B* **80** 094525
- [20] Zhao L *et al* 2010 arXiv:1002.0120
- [21] Doiron-Leyraud N *et al* 2007 *Nature* **447** 565
- [22] Taillefer L 2009 *J. Phys.: Condens. Matter* **21** 164212
- [23] Harrison N *et al* 2009 *J. Phys.: Condens. Matter* **21** 322202
- [24] Chakravarty S and Kee H Y 2008 *Proc. Natl Acad. Sci. USA* **105** 8835
- [25] Lin J and Millis A J 2005 *Phys. Rev. B* **72** 214506
- [26] Reznik D *et al* 2006 *Nature* **440** 1170
- [27] d’Astuto M *et al* 2008 *Phys. Rev. B* **78** R140511
- [28] Pintschovius L *et al* 2004 *Phys. Rev. B* **69** 214506
- [29] McQueeney R J *et al* 1999 *Phys. Rev. Lett.* **82** 628
- [30] Pintschovius L *et al* 2003 arXiv:cond-mat/0308357
- [31] Chung J H *et al* 2003 *Phys. Rev. B* **67** 014517
- [32] Braden M *et al* 2001 arXiv:cond-mat/0107498
- [33] Braden M *et al* 2002 *Physica C* **378–381** 89
- [34] Kaneshita *et al* 2002 *Phys. Rev. Lett.* **88** 115501